communications biology

A Nature Portfolio journal

Article

https://doi.org/10.1038/s42003-026-10274-0

GlycoAvatars: bead-coated membrane models for studying the cancer-immune cells interactome

Andreia Miranda[1,2], Marta Relvas-Santos[1,2], Camila Lourenço[1,2], Eduardo Ferreira[1,2], Diogo M. Cunha[3,4,5], Carlos Palmeira[1,6,7], Lúcio Lara Santos[1,2,6,8], Pieta K. Mattila[3,4,5] & José Alexandre Ferreira[1,2,9]

Immature protein *O*-glycosylation, characterized by the Tn antigen expression rather than complex glycans, is prevalent in advanced solid tumors and promotes immune evasion. We developed GlycoAvatars, magnetic beads coated with plasma-membrane glycoproteins from glycoengineered cancer cells reflecting these alterations, to identify cancer-immune cell interactomes. We uncovered numerous membrane and intracellular proteins involved in glycan-mediated immune signaling, providing a novel high-throughput strategy for identifying potential relevant molecular nodes foreseeing therapeutic targets.

The ability of tumors to progress and evade immune surveillance is frequently mediated by aberrant protein glycosylation characterized by glycosites carrying a single GalNAc residue (Tn antigen). These alterations enable tumor cells to exploit immune checkpoints, disrupt antigen presentation, and reprogram antigen-presenting cells towards more tolerogenic and immunosuppressive phenotypes[1]. However, the immune cell receptors and downstream signaling events driving immune suppression remain poorly understood, limiting insights into cancer-immune crosstalk and the development of novel immune checkpoint strategies. Here, we introduce GlycoAvatars, a platform that enables proteomic interrogation of immune contact interfaces formed in response to cancer-associated immature glycosylation. This approach allows the identification of candidate receptors, co-recruited signaling partners and interaction networks involved in glycan-dependent immune modulation, with implications for immune checkpoint biology and therapeutic targeting.

Results

To investigate glycan-mediated interactions, we developed GlycoAvatars, a platform employing magnetic beads coated with plasma membrane-derived glycoproteins isolated from glycoengineered cancer cells with immature glycosylation (Fig. 1a). Plasma membrane proteins were obtained from cancer cells by differential ultracentrifugation and enriched for Tn-bearing glycoproteins by VVA lectin pulldown (Supplementary Figs. 1 and 2a). To ensure that subsequent interactions were driven predominantly by *O*-glycans, membrane fractions were first treated with PNGase F to remove *N*-glycans. Efficient *N*-deglycosylation was confirmed by almost complete loss of Con A reactivity (Supplementary Fig. 2b). The resulting VVA-bound proteins were used to coat magnetic beads, generating the GlycoAvatars to interrogate the immune cells' interactome. This approach preserves native receptor conformation and co-receptor associations. GlycoAvatars were generated from *C1GALT1* knockout (KO) AGS (gastric cancer) and SW480 (colorectal cancer) cells, exhibiting homogenous Tn antigen expression in contrast to the extended glycosylation found in wild-type (WT) cells (Fig. 1b–d). Since WT do not express the Tn antigen and yield only residual protein recovery after VVA pulldown (Supplementary Fig. 2a), whole membrane extracts were elected as controls for bead coating. Nevertheless, WT-derived GlycoAvatars provide a reference condition with fully extended *O*-glycans[2,3], enabling direct comparison with the Tn-GlycoAvatars. Notably, proteomics analysis of the fractions used for GlycoAvatar generation revealed a substantial overlap between WT and KO preparations and a largely conserved membrane proteome (Supplementary Fig. 3 and Supplementary Data 1). Moreover, Gene Ontology (GO) profiling showed that the protein extracts were enriched in extracellular components (membrane or secreted), as supported by quantitative intensity analysis

[1]Experimental Pathology and Therapeutics Group, Research Center of IPO-Porto (CI-IPOP)/RISE@CI-IPOP (Health Research Network), Portuguese Oncology Institute of Porto (IPO-Porto)/Porto Comprehensive Cancer Center Raquel Seruca (Porto.CCC Raquel Seruca), Porto, Portugal. [2]School of Medicine and Biomedical Sciences Abel Salazar (ICBAS), University of Porto, Porto, Portugal. [3]Institute of Biomedicine, and MediCity Research Laboratories, University of Turku, Turku, Finland. [4]Turku Bioscience, University of Turku and Åbo Akademi University, Turku, Finland. [5]InFLAMES Research Flagship, University of Turku, Turku, Finland. [6]Health School of University Fernando Pessoa, Porto, Portugal. [7]Department of Immunology, Portuguese Oncology Institute of Porto (IPO-Porto), Porto, Portugal. [8]Department of Surgical Oncology, Portuguese Oncology Institute of Porto (IPO-Porto), Porto, Portugal. [9]GlycoMatters Biotech, Espinho, Portugal. e-mail: jose.a.ferreira@ipoporto.min-saude.pt

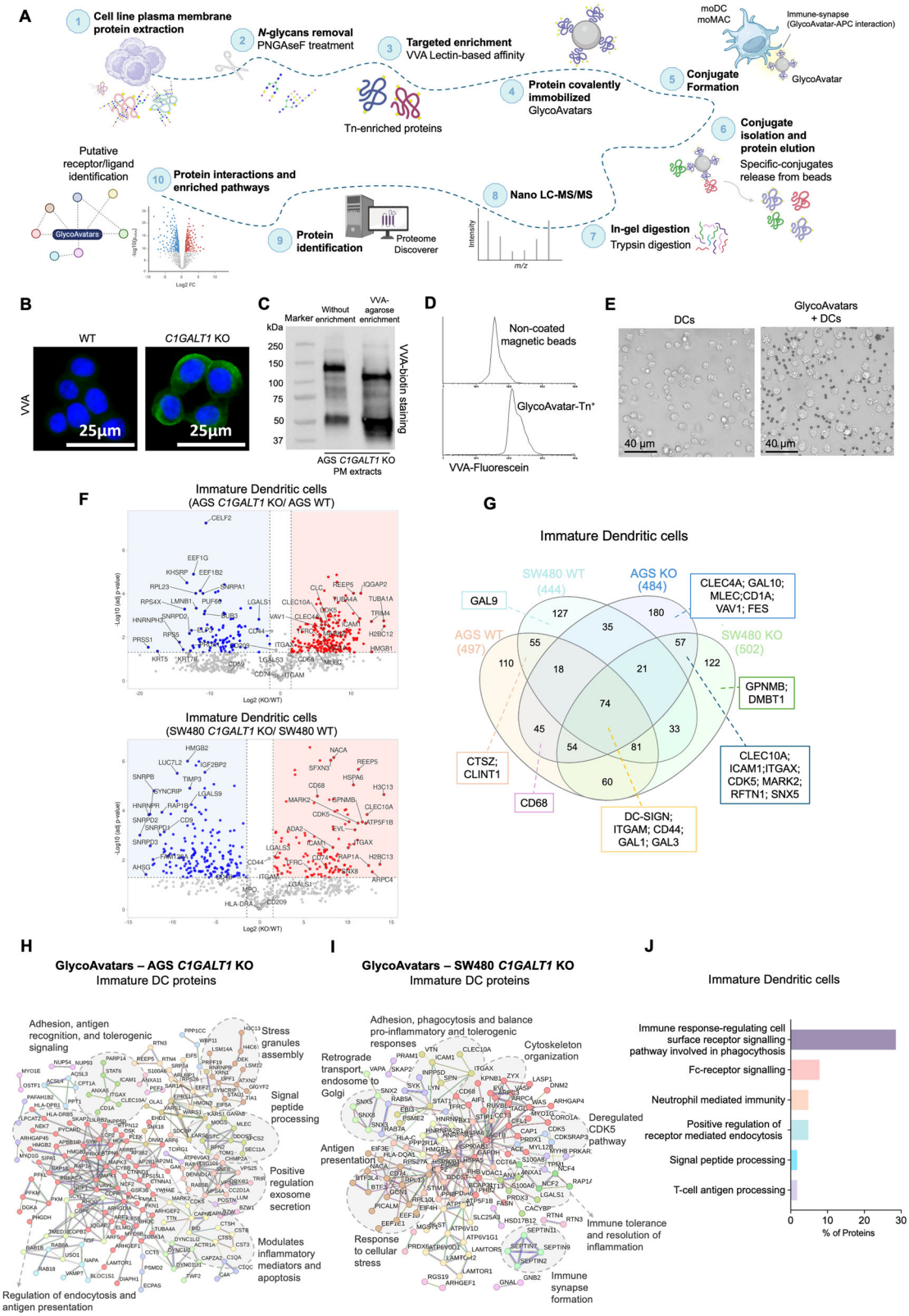

(Supplementary Fig. 4a, b and Supplementary Data 1). Importantly, comparative proteomic profiling revealed that AGS- and SW480-derived GlycoAvatars display markedly distinct membrane compositions in both WT and Tn^+ conditions, reflecting relevant cell line specific proteomic contexts (Supplementary Fig. 5a). Also, AGS-derived membranes were predominantly enriched in pathways related to immune defense, ligand scavenging and adhesion-associated cell death (Supplementary Fig. 5b). On the other hand, SW480-derived membranes preferentially associated with heme handling, metabolic and cellular stress responses, and cytoskeletal signaling (Supplementary Fig. 5c). Together, these data show that AGS- and SW480-derived GlycoAvatars retain distinct membrane contexts despite homogeneous immature glycosylation. Accordingly, the platform captures

Fig. 1 | Roadmap for identifying glycoprotein-mediated contact interfaces between immune cells and engineered GlycoAvatars. A Workflow overview. Plasma membrane proteins from glycoengineered cancer cell lines (AGS and SW480 *C1GALT1* KO) reflecting a cancer-associated *O*-glycome were *N*-deglycosylated and enriched using VVA lectin affinity chromatography to isolate Tn-enriched glycoproteins. These proteins were immobilized on magnetic beads to form GlycoAvatars and validated by flow cytometry. GlycoAvatars were incubated with DCs or MACs. Unbound cells were removed by washing. Associated protein complexes were recovered, digested, analyzed by mass spectrometry, and subjected to bioinformatics for protein identification and pathway analysis. Panel A created with BioRender.com. **B** Glycoengineered cancer cell lines. AGS and SW480 *C1GALT1* KOs served as cancer-associated Tn antigen sources. **C** Tn-glycoprotein enrichment. Plasma membrane proteins were enriched using VVA lectin to isolate Tn-bearing glycoproteins. **D** GlycoAvatars development. Successful glycoprotein coating and Tn antigen presence on GlycoAvatars were confirmed via flow cytometry. **E** Structured contact interface formation. Interaction between DCs or MACs and GlycoAvatars was validated using bright-field microscopy. **F** Identification of contact interface-enriched proteins. Volcano plots revealed significantly interface-enriched proteins, including CLEC10A, detected exclusively in KO-GlycoAvatars across donors ($n = 3$). **G** Protein distribution. A Venn diagram shows proteins enriched in GlycoAvatar-iDC interactions. **H** Functional enrichment. Enriched pathways and networks of DC-specific proteins interacting with KO-GlycoAvatars are shown for AGS (**I**) and SW480 (**J**) models. Protein abundance was estimated by MS-intensity-based label-free quantification. Only proteins fulfilling $\log_2FC > 2$, adjusted $p < 0.05$ and detected in three biological replicates after subtraction of bead-only and coated-bead backgrounds were included.

glycan-dependent interactions involving Tn-bearing membrane glycoproteins across different tumor backgrounds, rather than the isolated Tn epitope.

GlycoAvatars were then exposed to immune cells (immature and mature dendritic cells -iDCs, mDCs and immature macrophages - iMACs) (Fig. 1e). Bright-field imaging confirmed the formation of structured bead-immune cell contact interfaces (Supplementary Fig. 6). Following incubation with immune cells, bound proteins were recovered by magnetic pull-down and identified by nanoLC-MS/MS[4]. Employing this methodology, we identified 416 proteins significantly enriched or exclusively expressed on the pull-downs from the GlycoAvatars of AGS and SW480 *C1GALT1* KO cells interacting with iDCs compared to GlycoAvatars with extended glycosylation (Fig. 1f, g and Supplementary Data 2). Notably, protein abundance was estimated by MS intensity-based label-free quantification. Differential enrichment was assessed using moderated *t*-tests with FDR correction after subtraction of bead-only and coated-protein background signals. Only proteins showing robust interaction-dependent enrichment ($\log_2$ fold-change >2; adjusted $p < 0.05$) and consistent detection across biological replicates were retained for downstream analyses. Approximately 60% were predicted to be plasma membrane-associated. Known Tn-binding lectins, such as CLEC10A (CD301 or MGL) and CLEC4A (DCIR), were identified, validating the approach[5]. In addition to these established Tn-recognizing receptors, the revised interactomes consistently revealed the co-recruitment of proteins with documented roles in membrane organization, cytoskeletal dynamics and immune synapse formation. In iDCs, these include SNX5[6], STAB1 (Stabilin-1)[7], ICAM1 (CD54)[8], ITGAX (CD11c)[9], MARK2 (PAR-1b/EMK)[10,11] and RFTN1 (Raftlin)[12], as well as GPNMB10[13], consistent with the assembly of a structured synapse-like contact interface (Fig. 1f, g and Supplementary Data 3). We also observed additional immune lectins, including MLEC[14] and GAL10[15]. To our knowledge, these proteins have not been previously implicated in Tn-driven immune synapses. STRING network analysis revealed both shared and cell line-specific interaction patterns (Fig. 1h, i), reflecting differences in the underlying membrane proteomes. The identification of STRING connectivity between membrane and intracellular components (Fig. 1h, i) supports the presence of an interface-associated signaling network. Despite these differences, pathway analysis revealed significant enrichment for biological processes related to receptor activation and antigen uptake, including phagocytosis, Fc-receptor signaling and receptor-mediated endocytosis (Fig. 1j), consistent with coordinated immune engagement. Together, these data indicate that GlycoAvatars capture immune contact interfaces composed of Tn-binding lectins and co-recruited membrane-associated and intracellular proteins. Across tumor models, a subset of interaction features and pathways is shared, consistent with common Tn-driven immune engagement mechanisms. In parallel, distinct interaction architectures reveal cell line-specific responses shaped by the underlying tumor membrane proteome.

We expanded our approach to compare the interactomes of iDCs with mDCs and iMACs, further demonstrating the technique's feasibility and applicability. We started by identifying proteins preferentially enriched in iDCs relative to mDCs. The objective was to capture interactomes specific to the immature DC state, where antigen recognition and immune tolerance are primarily established (Fig. 2a and Supplementary Fig. 7). Analysis of iDC-enriched proteins revealed minimal overlap between AGS- and SW480-derived GlycoAvatars, with CLEC10A as the only shared protein (Supplementary Fig. 7a). Focused quantitative plots further illustrated that CLEC10A was enriched in conjugates formed with Tn$^+$ GlycoAvatars, with stronger enrichment in iDCs than in mDCs (Supplementary Fig. 7b and Supplementary Data 3). Nevertheless, most enriched proteins were cell-line-specific, supporting a context-dependent engagement of immature DCs. Pathway enrichment analysis further showed that, despite distinct protein-level interactomes, both models converged on immune recognition and uptake processes, including C-type lectin signaling, phagocytosis and endocytic pathways (Supplementary Fig. 7c). Nevertheless, AGS-derived GlycoAvatars engage iDCs through interaction programmes dominated by active phagocytic uptake reminiscent of pathogen handling, whereas SW480-derived GlycoAvatars engage iDCs through more regulated endocytic sampling and membrane trafficking pathways. Thus, despite a common Tn-rich glyco-state, the resulting immune interactomes remain strongly shaped by cancer cell-specific membrane proteomes. Collectively, the cancer cell proteome context determines how iDCs decode and process identical truncated O-glycan signals. We then focused on proteins selectively enriched in mature DCs to delineate interaction programmes that emerge upon maturation (Fig. 2a and Supplementary Data 3). In this context, CLEC10A and CLEC4A showed reduced enrichment in mDCs, consistent with well-described downregulation during DC maturation. Across both tumor models, mDC interactomes were enriched for pathways linked to negative regulation of type I interferon signaling, suggesting immune suppression cues mediated by the Tn antigen. Cell-type-specific differences were also observed: AGS cells showed enrichment in IL-10 production and Type-1 helper responses, while SW480 cells showed enrichment in B-cell differentiation pathways (Fig. 2b). Common proteins consistently mediating key immune processes related to tumor dynamics included ICAM1/CD54 (cell adhesion and immune activation) and TFRC/CD71 (antigen capture and metabolism), were identified across both cell types (Fig. 2c)[16–18]. Quantitative plots further illustrated that ICAM1 and TFRC were enriched in both iDC and mDC conjugates formed with Tn$^+$ GlycoAvatars from both cell lines, with stronger enrichment in mDCs than in iDCs (Supplementary Fig. 8 and Supplementary Data 3). In iMACs interacting with GlycoAvatars-Tn +, we identified 106 proteins (Fig. 2d and Supplementary Data 4), with some membrane proteins being common to iDCs (Fig. 2e), highlighting their role in Tn antigen recognition and APC modulation. Key iMAC-enriched proteins included RHOC, CFL1, MARK2, GPNMB and PSTPIP2 (Supplementary Fig. 9 and Supplementary Data 5), involved in cytoskeletal rearrangement, antigen uptake, inflammatory response modulation, and M1/M2 polarization[19,20] (Fig. 2f, g). Notably, while iDC interactomes were dominated by recognition- and uptake-associated programmes consistent with antigen sampling and tolerogenic priming (Fig. 1h, i). On the other hand, iMACs preferentially assembled cytoskeleton and polarization-linked networks (Fig. 2f), highlighting APCs' specific decoding of identical tumor glyco-interfaces. Together, these observations underscore the context-dependent nature of

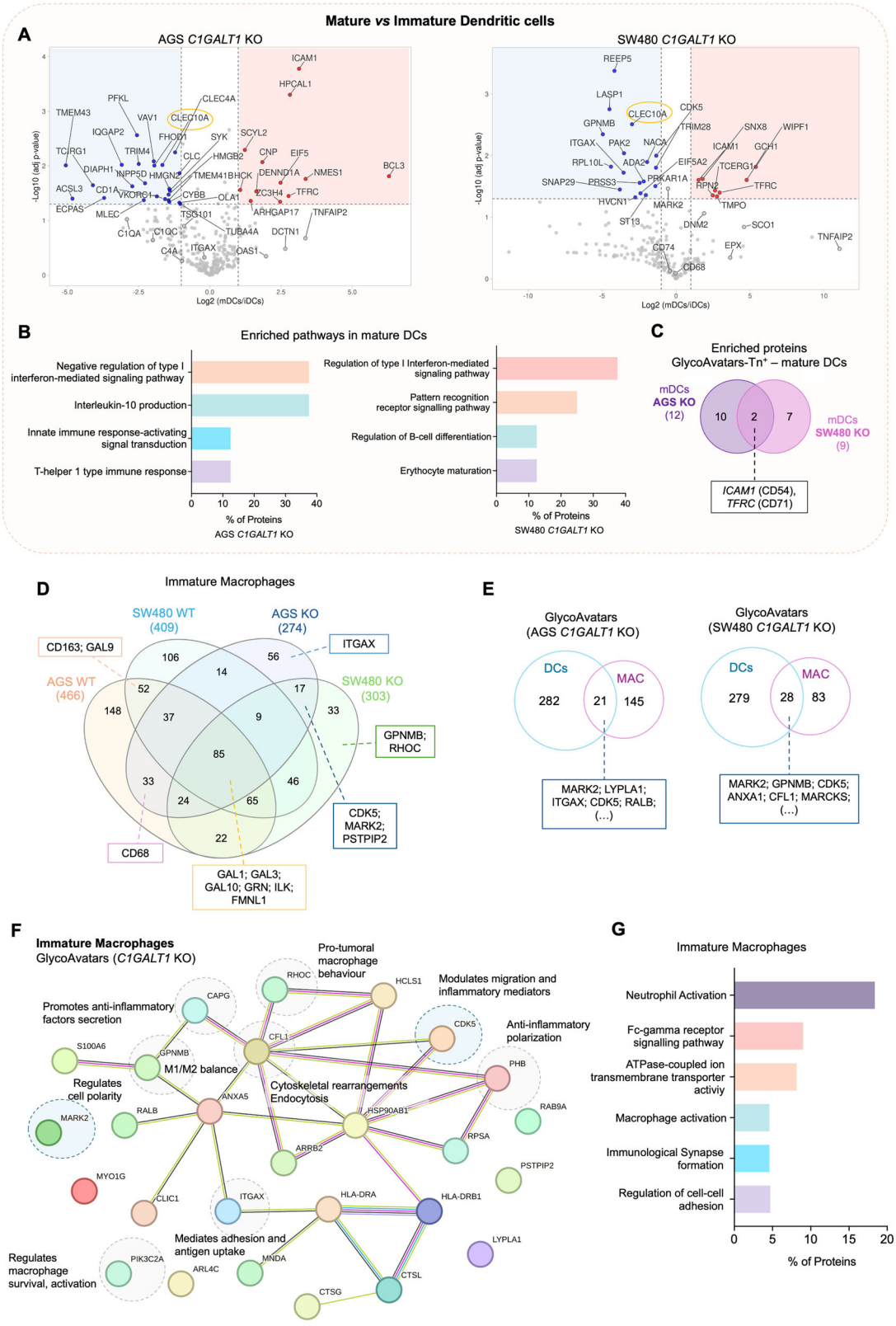

glycan-driven immune engagement and the capacity of the GlycoAvatars platform to resolve APCs' specific interactomes.

Discussion

GlycoAvatars represent a discovery-oriented platform designed to preserve aspects of native receptor conformation and co-receptor association, offering a more context-preserving model for dissecting the complex interplay between cancer glycosylation and the immune system. Its versatility enables the incorporation of diverse glycans and glycoproteoforms, supporting systematic mapping of glycan-mediated interactomes across distinct immune cell states. The key conceptual advance of GlycoAvatars lies in enabling proteomic isolation of immune contact interfaces formed in

Fig. 2 | Identification and characterization of proteins mediating GlycoAvatar-immune cell contact interfaces using mass spectrometry. A Differential protein expression between DC maturation states. Comparative analysis of protein abundances in mDCs versus iDCs revealed maturation state-specific proteins. For instance, CLEC10A was more abundant in iDC-GlycoAvatar conjugates than in mDC-GlycoAvatar conjugates, consistent with literature reports that CLEC10A expression is higher in iDCs. Blue arrows indicate relevant downregulated proteins, orange arrows represent non-significantly changed proteins, and red arrows highlight upregulated proteins in mDCs. **B** Enriched pathways in mDC interactions. Proteins significantly enriched in mDC interactions with AGS and SW480 GlycoAvatars were associated with biological pathways such as negative regulation of type I interferon signaling, innate immune signaling, and other immune regulatory processes. **C** Common proteins across cell lines. Among the proteins enriched in mDC interactions with AGS (12 proteins) and SW480 (9 proteins) GlycoAvatars, 2 proteins were common, highlighting shared mechanisms in the Tn-specific contact interfaces. **D** Venn diagram depicting protein distribution from GlycoAvatar-immature macrophage interactions. Proteins exclusive to AGS/SW480 GlycoAvatars-iMACs conjugates highlight specific interactions driven by Tn-enriched glycoproteins, whereas those exclusive to WT-GlycoAvatar conjugates reflect interactions associated with the native *O*-glycome. **E** Summary of DC- and MAC-specific proteins from GlycoAvatars. Venn diagrams highlight the overlap and exclusivity of proteins identified in iDCs and iMACs interacting with AGS and SW480 KO GlycoAvatars. **F** Protein-protein interaction network of MAC-specific proteins from GlycoAvatars. STRING-based analysis of MAC-specific proteins revealed key regulators of macrophage polarization (RHOC, MARK2), migration (PSTPIP2, CDK5), and cytoskeletal dynamics (CFL1, ITGAX). **G** Functional enrichment of MAC-specific proteins. Enriched pathways and biological processes from MAC-specific proteins interacting with GlycoAvatars. Protein abundance was estimated by MS-intensity-based label-free quantification. Only proteins fulfilling $\log_2FC > 2$, adjusted $p < 0.05$ and detected in three biological replicates after subtraction of bead-only and coated-bead backgrounds were included.

response to altered glycosylation, thereby supporting the identification of candidate glycan-dependent interaction networks. Compared with glycan or glycopeptide microarray[21,22] and synthetic glycodendrimers[23,24], which assess binding to isolated motifs, GlycoAvatars display the complete engineered tumor glycoproteome in a defined glyco-state. This configuration preserves a broader membrane-associated context, including protein scaffold diversity and aspects of membrane topology and co-receptor organization. As such, GlycoAvatars capture glycan-dependent interactions involving Tn-bearing membrane glycoproteins in a broader membrane context, not the isolated Tn epitope. In contrast to ligand-based receptor capture[25,26] or bioorthogonal click-chemistry approaches[27,28], this platform does not rely on a single soluble ligand or metabolic labeling. Importantly, GlycoAvatars complement existing methods, including receptor-centric proximity labeling strategies (*e.g.* BioID[29], APEX[30], EMARS[31]), by enabling direct proteomic interrogation of the immune-membrane interface. This allows the capture of candidate molecular assemblies formed through glycan-dependent recognition, without requiring genetic modification of immune cells. Moreover, unlike whole cell co-culture systems, GlycoAvatars decouple ligand presentation from cell-intrinsic variables, enabling focused proteomic analysis of the immune membrane-GlycoAvatar interface. Importantly, GlycoAvatars also have relevant limitations. The platform does not discriminate direct glycan-binding receptors from co-recruited membrane partners or proximal signaling components, and it does not by itself provide a direct functional readout of immune activation. Accordingly, the resulting interactomes should be interpreted as candidate molecular assemblies rather than definitive evidence of direct glycan-receptor engagement. By identifying membrane and intracellular proteins engaged in glycan-dependent contacts, GlycoAvatars provide a hypothesis-generating framework to prioritize candidate interactions for downstream mechanistic and translational investigation. Notably, the isolated membrane-immune cell interactomes encompass both primary glycan-binding receptors and co-recruited signaling assemblies. This paves the way for a more physiologically grounded, systems-level view of glycan-dependent interfaces, potentially aligned with immune synapse-associated architectures. Although this approach does not yet assign definitive functional roles to individual glycoproteins, it establishes a rational framework for targeted perturbation and receptor-level validation. In summary, within these boundaries, GlycoAvatars offer a useful discovery platform for uncovering candidate glycan-dependent immune interactions that can be explored by orthogonal functional and mechanistic approaches.

Methods

C1GALT1 knockout models

C1GALT1 knockout (KO) cell lines derived from AGS and SW480 cells were generated using a CRISPR-Cas9–based approach as previously described by Freitas et al.[32] and Soares et al.[2]. Briefly, cells were transfected with Cas9 and guide RNAs targeting the exon (GTAAAGCAGGGCTACATGAG) of *C1GALT1*. Clonal populations were obtained by limiting dilution. Genomic editing was verified by Sanger sequencing of the targeted locus. Functional knockout of *C1GALT1* was confirmed by enhanced *Vicia villosa* (VVA) lectin (Vector Laboratories) binding and loss of core-1 elongation, as assessed by the Peanut agglutinin (PNA) lectin (Vector Laboratories) before and after sialidase treatment.

Plasma-membranes isolation

Plasma membrane proteins were isolated by differential centrifugation. Cells were scraped from T300 flasks in hypotonic lysis buffer (20 mM HEPES, pH 7.4, 10 mM KCl, 2 mM $MgCl_2$, 1 mM EDTA, 1 mM EGTA, supplemented with protease and phosphatase inhibitors) and incubated on ice for 15 min. Cells were then mechanically disrupted by repeated passage through a 27-gauge needle. The homogenate was centrifuged at 720 × *g* for 5 min at 4 °C to remove nuclei and unbroken cells. The resulting supernatant was further centrifuged at 10,000 x *g* for 5 min at 4 °C to pellet mitochondria and other large organelles. The clarified supernatant was subsequently subjected to ultracentrifugation at 100,000 × *g* for 60 min at 4 °C to isolate membrane fractions. The membrane pellet was resuspended in 1 mL of lysis buffer, passed ten times through a 25-gauge needle, and centrifuged again at 100,000 × *g* for 45 min at 4 °C. The final pellet was resuspended in 20 mM Tris-buffered saline (TBS) containing 0.1% sodium dodecyl sulfate (SDS) and subjected to three cycles of sonication (5 min at 40 °C followed by 5 min on ice). Following protein solubilization, samples were centrifuged at 10,000 × *g* for 10 min at 4 °C, and the supernatant was collected for downstream analyses.

Glycoproteins isolation

Plasma membrane proteins were extracted, quantified, and adjusted to 300 µL with TBS-0.3% SDS and 15 µL of 20% NP-40. Proteins were deglycosylated overnight at 37 °C with PNGase F (2 U per 20 µg protein), followed by enzyme inactivation at 95 °C for 20 min. The efficiency and specificity of *N*-glycan removal were confirmed by lectin blotting using biotinylated-concanavalin A (Con A-biotin, Vector Laboratories). Samples were then diluted to 400 µL with LacA buffer (20 mM Tris, pH 7.4, 150 mM NaCl, 1 mM Urea, 0.1 M $CaCl_2$, 0.1 M $MgCl_2$, 0.1 M $MnCl_2$, 0.1 M $ZnCl_2$), incubated with 100 µL VVA-agarose (Vector Laboratories) for 30 min, then washed and eluted with 3% acetic acid. Eluates were dried using a SpeedVac and reconstituted in TBS-0.3% SDS. Enrichment for Tn-glycosylated proteins was validated by lectin blotting using biotinylated-VVA (VVA-biotin, Vector Laboratories).

Western blotting

Whole-cell lysates and plasma membrane extracts were resolved on 4–20% precast polyacrylamide gels and transferred onto 0.45-µm nitrocellulose membranes. Membranes were blocked with Carbo-Free Blocking Solution (1×) for 90 min and subsequently incubated for 60 min with either VVA-biotin (1:10,000 dilution in PBS-T containing 50% (v/v) blocking solution) or Con A-biotin (1:10,000 dilution in TBS-T containing 50% (v/v) blocking

solution supplemented with 1 mM $CaCl_2$ and 1 mM $MgCl_2$). Lectin binding was detected using the VECTASTAIN Elite ABC Peroxidase Kit, followed by chemiluminescent detection with Amersham ECL Prime.

GlycoAvatars development

Dynabeads™ M-450 Tosyl-activated (20×10^6) (ThermoFisher Scientific) were washed twice with 0.1 M phosphate buffer (pH 7.4) and incubated with 10 µg of target membrane proteins for 1.5 h at room temperature with agitation (1000 rpm). Phosphate buffer containing 0.1% BSA was then added, and the beads were incubated overnight at 37 °C to ensure binding. The beads were washed with 20 mM HEPES and incubated for 2 h at room temperature with 25 mM bis(sulfosuccinimidyl)suberate (BS3) crosslinker (ThermoFisher Scientific), followed by washing with 0.2 M Tris buffer (pH 8.5) containing 0.1% BSA and overnight incubation to deactivate residual tosyl groups. The beads were then washed with PBS containing 0.1% BSA and 2 mM EDTA (pH 7.4). The binding of Tn-enriched glycoproteins was confirmed by flow cytometry using VVA-FITC (Vector Laboratories), and wild-type proteins' binding was confirmed using anti-Pan Cytokeratin-Alexa Fluor 647 (NBP2-34394AF647).

Microscopy of GlycoAvatar-immune cells contact interfaces

After coupling and washing, GlycoAvatars were incubated with immune cells under standard culture conditions. Cell-bead interactions were visualized by bright-field microscopy. Images were acquired to directly assess bead attachment at the cell surface and the formation of structured contact interfaces. Structured contacts were defined as bead-cell interfaces displaying close membrane apposition and stable bead positioning at the cell surface.

GlycoAvatars-immune cells complexes and synapse isolation

Dendritic cells or macrophages were resuspended in phenol red–free RPMI medium and combined with GlycoAvatars at a 1:1 ratio, followed by incubation for 60 min at 37 °C with agitation (1000 rpm). Conjugation was confirmed microscopically, and the complexes were washed with cold CSK buffer (300 mM sucrose, 100 mM sodium chloride, 10 mM PIPES, pH 6.8, 3 mM magnesium chloride) to remove unbound cells. The conjugates were then resuspended in CSK buffer containing 0.5% Triton X-100 and protease/phosphatase inhibitors, sonicated, and repeatedly washed with CSK buffer supplemented with 0.5% Triton X-100 to remove cellular debris. Bound proteins were eluted with 25 µL Laemmli buffer at 70 °C for 30 min (1000 rpm) and subsequently processed by SDS-PAGE and in-gel digestion.

MS sample preparation

Eluates from GlycoAvatars–immune cell protein complexes were identified using a bottom-up proteomics strategy by nanoLC-HCD-MS/MS. Briefly, isolated proteins were loaded onto SDS–PAGE gels and visualized using a Zinc Reversible Stain Kit. Gel bands were excised into 1–2 mm pieces, destained in Tris–glycine buffer (pH 8.0), and washed three times with ultrapure water for 10 min each. Gel pieces were dehydrated with LC–MS-grade acetonitrile (ACN) and disulfide bonds were reduced with 20 mM dithiothreitol (DTT) at 56 °C for 30 min, followed by dehydration with 100% ACN. Gel pieces were then rehydrated and alkylated with 55 mM iodoacetamide (IAA) for 20 min in the dark to prevent disulfide bond reoxidation. After washing with 100 mM ammonium bicarbonate and further dehydration, in-gel digestion was performed overnight at 37 °C in a humid chamber using trypsin (0.02 µg μL^{-1} in 40 mM ammonium bicarbonate/10% ACN). Digestion was quenched with 100% ACN. Peptides were extracted twice with 50% ACN / 5% formic acid (FA) for 20 min each, and pooled extracts were dried using a SpeedVac prior to LC–MS/MS analysis.

LC-MS/MS data acquisition

For protein identification, peptides were loaded into a Vanquish Neo UHPLC system coupled with a QExactive Plus Hybrid Quadrupole-Orbitrap mass spectrometer (Thermo Fisher Scientific), which was fitted with a nano-electrospray ion source (EASY-Spray source; Thermo Fisher Scientific). Mobile phases were 0.1% FA in ultrapure water (eluent A) and 0.1% FA in 80% ACN (eluent B). A 10 µL sample was injected into a trapping column (C18 PepMap Neo, 5 µm particle size 300µm × 5 mm) and separated on an analytical column (EASY-Spray C18 PepMap, 100 Å, 75 µm × 150 mm, 3 µm particle size) at 0.25 µL min^{-1} and 35 °C. Peptide separation used a gradient of 2.5%–12% B over 7 min, 12%–46% B over 50 min, and 46%–99% B over 5 min, holding at 99% B for 10 min. Mass spectrometry operated in positive ion mode (m/z 300–2000) with a 1.9 kV spray voltage and 275 °C capillary temperature. Full MS settings included a 140,000 resolution, AGC target of 3×10^6, and 200 ms maximum injection time, with the 15 most intense ions selected for higher energy collisional dissociation (HCD) with NCE of 30%. Data were recorded with Xcalibur (v4.5).

Protein annotation and quantification

Whole-cell, subcellular and GlycoAvatars-interactome proteomic datasets were processed in Proteome Discoverer 3.1 using the SequestHT search engine and Percolator against the SwissProt human proteome database (accessed October 22, 2023). Search parameters included trypsin specificity with up to two missed cleavages, a 10-ppm precursor-ion tolerance and a 0.02-Da fragment-ion tolerance, carbamidomethyl-cysteine as a fixed modification (+ 57.021 Da) and methionine oxidation as a variable modification (+ 15.995 Da). Protein groups supported by fewer than two unique peptides or not passing high-confidence FDR thresholds were excluded from downstream analyses. Gene-ontology (GO) annotation for cellular compartment, molecular function and biological processes was performed in Proteome Discoverer 3.1. Protein abundance was quantified using label-free MS1-intensity derived precursor areas. Differential protein abundance was expressed as $\log_2$ fold-change between the relevant experimental conditions for each comparison. Statistical significance was assessed using moderated t-tests with FDR correction. Proteins were considered significantly enriched when $\log_2 FC > 1.5$, adjusted $p < 0.05$ and detected in three biological replicates. These thresholds were applied consistently across volcano plots and Venn diagrams.

GlycoAvatars interactome analysis

For the GlycoAvatars interactome analysis, proteins detected in bead-only controls and in GlycoAvatars coated with membrane proteins but incubated without immune cells were considered background and excluded from further analysis. This filtering step minimizes non-specific protein carryover, and only proteins consistently enriched upon immune-GlycoAvatar engagement were retained for interactome profiling. Differential enrichment and statistical testing followed the quantitative framework described above. Proteins retained after differential filtering were further analyzed in STRING v12.0 to examine protein–protein interaction networks, functional associations and REACTOME pathways. Enriched biological processes were visualized in Cytoscape (v3.10.2) using the ClueGO plugin, applying a significance threshold of $p \leq 0.05$, a GO-tree interval of 4–10 and a kappa score of 0.64 for pathway clustering.

Statistics and reproducibility

At least three biologically independent experiments were performed unless stated otherwise. Statistical analyses were performed using R and GraphPad Prism. P-values for Volcano plots were calculated using an unpaired two-tailed Student's t-test. For bar plots, data are presented as mean ± standard deviation (SD). Statistical details for each experiment are provided in the corresponding figure legends.

Reporting summary

Further information on research design is available in the Nature Portfolio Reporting Summary linked to this article.

Data availability

All data supporting the findings of this study are available within the paper and its Supplementary Information. The numerical source data underlying all graphs can be found in Supplementary Data. The protein mass spectrometry data generated in this study have been deposited in the PRIDE repository under accession code PXD060750.

Received: 27 January 2025; Accepted: 6 May 2026;
Published online: 15 May 2026

References

1. Cornelissen, L. A. M. et al. Tn antigen expression contributes to an immune suppressive microenvironment and drives tumor growth in colorectal cancer. *Front. Oncol.* **10**, 1622 (2020).
2. Soares, J. et al. CD276 immature glycosylation drives colorectal cancer aggressiveness and T cell mediated immune escape. *Cell Commun. Signal*. https://doi.org/10.1186/s12964-026-02672-y (2026).
3. Fernandes, E. et al. Nucleolin-Sle A glycoforms as E-selectin ligands and potentially targetable biomarkers at the cell surface of gastric cancer cells. *Cancers* **12**, 861 (2020).
4. Cunha, D. M., Hernández-Pérez, S. & Mattila, P. K. Isolation of the B cell immune synapse for proteomic analysis. *Methods Mol. Biol.* **2654**, 393–408 (2023).
5. Reis e Sousa, C., Yamasaki, S. & Brown, G. D. Myeloid C-type lectin receptors in innate immune recognition. *Immunity* **57**, 700–717 (2024).
6. Cabrera-Reyes, F. et al. SNX5 promotes antigen presentation in B cells by dual regulation of actin and lysosomal dynamics. *Life Sci. Alliance* **8**, e202402917 (2025).
7. Kzhyshkowska, J. Multifunctional receptor stabilin-1 in homeostasis and disease. *ScientificWorldJournal* **10**, 2039–2053 (2010).
8. Bui, T. M., Wiesolek, H. L. & Sumagin, R. ICAM-1: a master regulator of cellular responses in inflammation, injury resolution, and tumorigenesis. *J. Leukoc. Biol.* **108**, 787–799 (2020).
9. Wu, J., Wu, H., An, J., Ballantyne, C. M. & Cyster, J. G. Critical role of integrin CD11c in splenic dendritic cell capture of missing-self CD47 cells to induce adaptive immunity. *Proc. Natl. Acad. Sci. USA* **115**, 6786–6791 (2018).
10. Deng, J. et al. LKB1-MARK2 signalling mediates lipopolysaccharide-induced production of cytokines in mouse macrophages. *J. Cell Mol. Med.* **24**, 11307–11317 (2020).
11. Hurov, J. B. et al. Immune system dysfunction and autoimmune disease in mice lacking Emk (Par-1) protein kinase. *Mol. Cell Biol.* **21**, 3206–3219 (2001).
12. Watanabe, A. et al. Raftlin is involved in the nucleocapture complex to induce poly(i:c)-mediated tlr3 activation. *J. Biol. Chem.* **286**, 10702–10711 (2011).
13. Prabata, A., Ikeda, K., Rahardini, E. P., Hirata, K.-I. & Emoto, N. GPNMB plays a protective role against obesity-related metabolic disorders by reducing macrophage inflammatory capacity. *J. Biol. Chem.* **297**, 101232 (2021).
14. Qin, S.-Y. et al. Malectin forms a complex with ribophorin I for enhanced association with misfolded glycoproteins. *J. Biol. Chem.* **287**, 38080–38089 (2012).
15. Kubach, J. et al. Human CD4+CD25+ regulatory T cells: proteome analysis identifies galectin-10 as a novel marker essential for their anergy and suppressive function. *Blood* **110**, 1550–1558 (2007).
16. Wirtz, S. et al. EBV-induced gene 3 transcription is induced by TLR signaling in primary dendritic cells via NF-kappa B activation. *J. Immunol.* **174**, 2814–2824 (2005).
17. Keppler, S. J. et al. The lack of WIP binding to actin results in impaired B cell migration and altered humoral immune responses. *Cell Rep.* **24**, 619–629 (2018).
18. Lee, S. M., Suk, K. & Lee, W. H. Myristoylated alanine-rich C kinase substrate (MARCKS) regulates the expression of proinflammatory cytokines in macrophages through activation of p38/JNK MAPK and NF-κB. *Cell Immunol.* **296**, 115–121 (2015).
19. Xu, J. & Lv, H. PSTPIP2 alleviates obesity associated adipose tissue inflammation and insulin resistance in diabetes mice through promoting M2 macrophage polarization via activation of PPARγ. *J. Diab. Complications* **37**, 108479 (2023).
20. Todosenko, N., Yurova, K., Vulf, M., Khaziakhmatova, O. & Litvinova, L. Prohibitions in the meta-inflammatory response: a review. *Front Mol. Biosci.* **11**, 1322687 (2024).
21. Palma, A. S. et al. Unravelling glucan recognition systems by glycome microarrays using the designer approach and mass spectrometry. *Mol. Cell. Proteom.* **14**, 974–988 (2015).
22. Blixt, O. et al. A high-throughput O-glycopeptide discovery platform for seromic profiling. *J. Proteome Res.* **9**, 5250–5261 (2010).
23. van der Meijs, N. L. et al. Ligand-specific tuning of CLEC10A signalling strength and dendritic cell responses through engagement of different GalNAc-containing glycan structures. *FEBS J*. https://doi.org/10.1111/febs.70317 (2025).
24. Percec, V. et al. Modular synthesis of amphiphilic Janus glycodendrimers and their self-assembly into glycodendrimersomes and other complex architectures with bioactivity to biomedically relevant lectins. *J. Am. Chem. Soc.* **135**, 9055–9077 (2013).
25. Sobotzki, N. et al. HATRIC-based identification of receptors for orphan ligands. *Nat. Commun.* **9**, 1519 (2018).
26. Frei, A. P., Moest, H., Novy, K. & Wollscheid, B. Ligand-based receptor identification on living cells and tissues using TRICEPS. *Nat. Protoc.* **8**, 1321–1336 (2013).
27. Stöckmann, H. et al. Glycan-mediated, ligand-controlled click chemistry for drug-target identification. *Chembiochem* **17**, 150–154 (2016).
28. Chen, W., Smeekens, J. M. & Wu, R. Systematic and site-specific analysis of N-sialoglycosylated proteins on the cell surface by integrating click chemistry and MS-based proteomics. *Chem. Sci.* **6**, 4681–4689 (2015).
29. Roux, K. J., Kim, D. I., Raida, M. & Burke, B. A promiscuous biotin ligase fusion protein identifies proximal and interacting proteins in mammalian cells. *J. Cell Biol.* **196**, 801–810 (2012).
30. Lam, S. S. et al. Directed evolution of APEX2 for electron microscopy and proximity labeling. *Nat. Methods* **12**, 51–54 (2015).
31. Kotani, N. et al. Biochemical visualization of cell surface molecular clustering in living cells. *Proc. Natl. Acad. Sci. USA* **105**, 7405–7409 (2008).
32. Freitas, R. et al. A multivalent CD44 glycoconjugate vaccine candidate for cancer immunotherapy. *J. Control. Release* **367**, 540–556 (2024).

Acknowledgements

We thank the Portuguese Foundation for Science and Technology (2022.12980.BD, SFRH/BD/146500/2019, 2022.08311.CEECIND; PTDC/MED-OUT/2512/2021), the Research Council of Finland (grants 337530, 357910, 339810), and Finnish Cultural Foundations.

Author contributions

A.M., D.M.C., P.K.M., and J.A.F. designed research; A.M., M.R.S., C.L., E.F., and C.P. performed research; A.M. and M.R.S. performed bioinformatic analysis; D.M.C, L.L.S., P.K.M., and J.A.F. contributed new reagents/analytic tools; A.M., M.R.S., C.L., C.P., and J.A.F. analyzed data; A.M. and J.A.F. wrote the paper. All authors revised the paper.

Competing interests

L.L.S. and J.A.F. are the founders of GlycoMatters Biotech. J.A.F. is also the CEO of the company. The remaining authors declare no competing interests.

Additional information

Supplementary information The online version contains supplementary material available at https://doi.org/10.1038/s42003-026-10274-0.

Correspondence and requests for materials should be addressed to José Alexandre Ferreira.

Peer review information *Communications Biology* thanks Sandra van Vliet and the other, anonymous, reviewer(s) for their contribution to the peer review of this work. Primary handling editor: Ophelia Bu. A peer review file is available.